

## Highlights

### **Offline and online parameter estimation of nonlinear systems: Application to a solid oxide fuel cell system**

Yashan Xing, Lucile Bernadet, Marc Torrell, Albert Tarancón, Ramon Costa-Castelló, Jing Na

- An offline tuning strategy is proposed to calibrate state-space and steady-state models for a SOFC system under multiple operation conditions such that the SOFC models for various operation conditions can be obtained.
- An adaptive optimal parameter estimation method is proposed to online estimate time-varying parameters in the SOFC models for each operation condition. As a consequence, the slowly time-varying material properties can be presented by the estimated parameters.
- Comparison and discussion about offline and online parameter estimation methods for a SOFC system are provided and experimentally validated.

# Offline and online parameter estimation of nonlinear systems: Application to a solid oxide fuel cell system <sup>★</sup>

Yashan Xing<sup>a</sup>, Lucile Bernadet<sup>b</sup>, Marc Torrell<sup>b</sup>, Albert Tarancón<sup>b,c</sup>, Ramon Costa-Castelló<sup>a</sup> and Jing Na<sup>d</sup>

<sup>a</sup>Institut de Robòtica i Informàtica Industrial, CSIC-UPC. C/ Llorens i Artigas 4-6, 08028 Barcelona, Spain

<sup>b</sup>Department of Advanced Materials for Energy, Catalonia Institute for Energy Research (IREC), Jardins de les Dones de Negre 1, 2nd Floor, 08930 Sant Adria de Besos, Barcelona, Spain

<sup>c</sup>ICREA, Passeig Lluís Companys 23, 08010 Barcelona, Spain

<sup>d</sup>Faculty of Mechanical and Electrical Engineering, Kunming University of Science and Technology, Kunming, 650500, China

## ARTICLE INFO

### Keywords:

Adaptive parameter estimation  
Optimization  
Solid oxide fuel cell  
Time-varying parameter

## ABSTRACT

In this paper, an offline tuning strategy and an online parameter estimation method are proposed to calibrate the solid oxide fuel cell mathematical model. The offline tuning strategy is developed in order to tune the model under various operation condition. First, the particle swarm optimization method with gradient-based search method is applied to tune unknown parameters in the state-space model and the steady-state model for each operation condition. Then, the sensitive parameters are expanded to the polynomial equations. Moreover, the reconstructed model including coefficients in the polynomial equations are determined by using the particle swarm optimization method with gradient-based search method for whole operation conditions. To show the slowly time-varying performance of a solid oxide fuel cell, an adaptive optimal learning law is proposed to online minimize a cost function with the information of the estimation error. The estimation error is extracted through several low-pass filters and simple algebraic calculation. Finally, the proposed offline tuning strategy and the developed online adaptive estimation method are verified by conducting experiments on a practical solid oxide fuel cell test bench.

## 1. Introduction

### 1.1. Motivation

Various renewable energy technologies have received increasing concerns due to serious environmental pollution and rapid traditional energy consumption. Fuel cells are considered as one of the most promising candidates, which have the property of high power density and zero-release of pollution gases. Based on the material of the electrolyte, fuel cells can be classified into different types, such as polymer electrolyte membrane fuel cells, direct methanol fuel cells, solid oxide fuel cells, etc [10]. Among them, the solid oxide fuel cell (SOFC) has advantages of high energy conversion efficiency and high tolerance to fuel impurities. The operation temperature of SOFC is between 600°C with 1000°C. During long-period operation, degradation might affect SOFC system due to the high temperature operation condition [18]. Therefore, the main obstacle for SOFC wide utilization is the relatively low reliability and durability.

In order to interpret and analyze the performance, reliable mathematical models of SOFC are required. Due to the complexity and nonlinearity of SOFC, linear models cannot provide essential information of the system performance. On the other hand, the detailed knowledge of the fuel cell structure may not be available and high-order models are not convenient for control design. To enhance the model accuracy for the control-oriented nonlinear model, model identification methods can be applied to tune the dominating structural model errors [20]. However, the nonlinearity leads to some difficulties to obtain transfer functions and state-space equations through the simple linear model identification method. Therefore, parameter estimation methods of model identification methods for the nonlinear system is mainly considered in order to understand how fuel cell systems work and to deal with model tuning.

### 1.2. Literature Review

To calibrate SOFC models, parameter estimation methods can be divided into two categories: off-line parameter estimation methods and on-line parameter estimation methods. Specifically, off-line parameter estimation methods are mainly dependent on optimization techniques. Evolutionary algorithms are a particular class of optimization techniques, which can be mainly classified into two types: conventional gradient-based search algorithms [21] and global stochastic optimization approaches. Gradient-based algorithms are used to find a local optimum based on the gradient information to determine the search direction. Global stochastic optimization approaches are non-gradient methods to determine a global optimum, which mainly include genetic

<sup>★</sup> This work was partially funded by the Spanish national project DOVELAR (ref. RTI2018-096001-B-C32) and the MCIN/AEI/10.13039/501100011033/ERDF/EU under grant (PID2021-126001OB-C31 (MAFALDA)). This work was partially funded by National Natural Science Foundation of China under grants (61922037) and (61873115), Yunnan Fundamental Research Projects under grant (202001AV070001) and Yunnan Major Scientific and Technological Projects under grants (202102AA310042) and (202202AG050002).

 yashan.xing@outlook.com (Y. Xing); lbernadet@irec.cat (L. Bernadet); mtorrell@irec.cat (M. Torrell); atarancón@irec.cat (A. Tarancón); ramon.costa@upc.edu (R. Costa-Castelló); najing25@163.com (J. Na)

algorithm (GA) [16, 4, 26], simulated annealing (SA) [17], differential evolution (DE) [6], particle swarm optimization (PSO) [9, 19, 27], etc. In [16], two different GAs were compared for tuning a fuel cell model. The results illustrated that the GA highly depended on the set range for each parameter. Yang *et al.* [26] proposed a modified genetic algorithm to tune a tubular SOFC model. The improved part is that a new fitness evaluation function was proposed and crossover was replaced with a reorganization strategy. The comparative results with the standard GA showed the effectiveness of the modified GA through the experimental data. In [4], the SOFC model was built by an artificial neural network and the GA was utilized to select the optimal parameters. However, there are some drawbacks existing in GA [27]. Especially, the efficiency degradation may happen in crossover and mutation when the tuning parameters are highly correlated. To address those drawbacks, the PSO algorithm inspired by the swarm behavior of animals has been widely used to tune unknown parameters in the fuel cell models. In [27, 19], a lumped parameter model of a fuel cell with some unknown constant parameters had been applied by PSO method in order to tune the model by using experiment data. Askarzadeh *et al.* [2] proposed an improved PSO method, where a new inertia weight function was proposed in order to enhance the convergence speed. More recently, Li *et al.* [11] proposed a hybrid PSO algorithm with adaptive inertial weight for achieving global search and local search. For each generation, the Broyden-Fletcher-Goldfarb-Shanno quasi-Newton method was used to do the local search. And a randomized regrouping strategy was used to regroup the generation for increasing the diversity. However, the above-mentioned optimization strategies are proposed to calibrate the mathematical model for the polarization curve under an operation condition such that the optimization strategies may not be suitable for different experimental data under various operation conditions.

Since evolutionary algorithms rely on the offline fitting procedures, unknown parameters cannot be estimated online. Moreover, material properties of a SOFC stack are slowly changing such that unknown model parameters are time-varying. In order to show the slowly time-varying performance of unknown parameters, adaptive parameter estimation methods have been widely used to achieve online parameter estimation for each operation condition, such as gradient descent algorithms [5], recursive least-squares (RLS) [23, 7]. In [23], the RLS method was used to estimate unknown parameters and fit the maximum power point curve of a fuel cell. In [7], constant parameters in the semi-empirical model of a fuel cell was estimated by the RLS method. More recently, the gradient descent algorithm was used to estimate slowly time-varying resistance in the equivalent circuit model for a fuel cell [5]. The main idea of these adaptive estimation methods is to minimize the output error and the robustness of these methods has been discussed in [12]. However, estimating time-varying parameters remains as an open and theoretically challenging issue [14, 15].

### 1.3. Contribution and Organization

The aim of this paper is to exploit an offline tuning strategy and an online parameter estimation method for a SOFC system in order to calibrate the mathematical model. To develop the offline tuning strategy for multiple operation conditions, the PSO method with gradient-based search method is first used to tune the state-space model and the steady-state model of a SOFC system for each operation condition, respectively. Then, sensitive parameters are expanded to the polynomial equations. Finally, the global model including coefficients in the polynomial equations are determined by using the PSO method with gradient-based search method again for whole operation conditions. For the online parameter estimation method to estimate unknown time-varying parameters, an adaptive optimal learning law is proposed to minimize a cost function with the information of the estimation error. The estimation error is extracted through several low-pass filters and simple algebraic calculation. Finally, the proposed methods are verified by conducting experiments on a practical SOFC test bench.

To this end, the main contributions of this paper are:

1. An offline tuning strategy is proposed to calibrate state-space and steady-state models for a SOFC system under multiple operation conditions such that the SOFC models for various operation conditions can be obtained.
2. An adaptive optimal parameter estimation method is proposed to online estimate time-varying parameters in the SOFC models for each operation condition. As a consequence, the slowly time-varying material properties can be presented by the estimated parameters.
3. Comparison and discussion about offline and online parameter estimation methods for a SOFC system are provided and experimentally validated.

The paper is organized as follows: The SOFC model and the problem formulation are given in Section 2. In Section 3 and Section 4, the offline global tuning strategy and the online parameter estimation method are proposed, respectively. Practical experiments and the method validation are presented in Section 5. Several conclusions are drawn in Section 6.

## 2. SOFC Model with Unknown Parameters

### 2.1. Description of SOFC

The SOFC is a sustainable energy conversion device that uses hydrogen and oxygen to produce electricity, thermal heat and water [10]. In this paper, a SOFC stack with 30 cells is taken into account. Figure 1 shows a practical SOFC system in the fuel cell laboratory of the Institut de Recerca en Energia de Catalunya (IREC). The dry hydrogen and the air as input gases enter into the SOFC. During the chemical reaction, unused gasses are directly released to the atmosphere and the generated steam water are reserved in the vessel. Since a SOFC stack operates at the high temperature, a preheat facility of the climatic chamber is required. Besides,

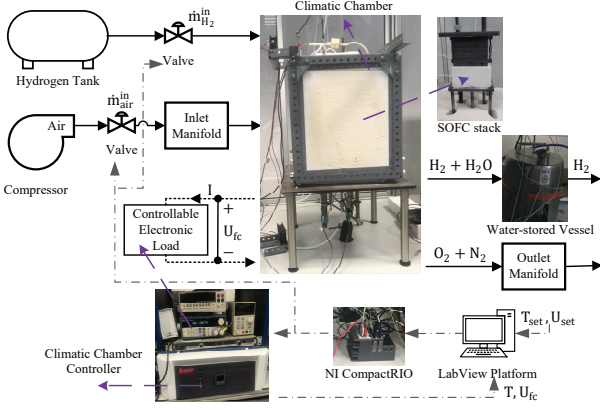


Figure 1: The SOFC test facility at IREC.

the climatic chamber can be used to regulate the temperature of the SOFC stack, including heating and cooling processes.

The detailed modelling and the control-oriented analysis of this SOFC system have been addressed in the recent work [25], where the mass balance model, the voltage balance model and the thermal energy balance model are introduced. In the following, a brief description of voltage and thermal energy models related to the parameter estimation will be provided in the following.

## 2.2. Mathematical Model of a SOFC system

The voltage balance of the SOFC is modeled as [25]:

$$U_{fc} = N_{cell} \cdot (U_{ner} - U_{act,ca} - U_{act,an} - U_{ohm} - U_{con}) \quad (1)$$

where  $N_{cell}$  denotes the number of cells.  $U_{ner}$  is the Nernst voltage, which is represented as

$$U_{ner} = \Delta U + f_1(T_{fc})$$

where  $\Delta U$  denotes the standard potential for each cell of SOFC. The nonlinear function  $f_1(T_{fc})$  is defined in Appendix A. Moreover, activation losses at the cathode and anode ( $U_{act,ca}, U_{act,an}$ ), Ohmic losses  $U_{ohm}$  and concentration losses  $U_{con}$  are three types of irreversible potential losses during the SOFC operation. They can be modeled as follows:

$$U_{ohm} = R_0 I_{fc} f_2(T_{fc})$$

$$U_{act,ca} = \frac{1}{\alpha_{ca}} T_{fc} f_3(I_{fc})$$

$$U_{act,an} = \frac{1}{\alpha_{an}} T_{fc} f_4(I_{fc})$$

$$U_{con} = T_{fc} f_5(I_{fc})$$

where the nonlinear functions from  $f_2$  to  $f_5$  are given in Appendix A. The constants of charge transfer for anode and cathode are  $\alpha_{an}$  and  $\alpha_{ca}$ , respectively.  $R_0$  represents the reference resistance determined by the experiment at the reference temperature  $T_0$ .

The lumped parameter model of the thermal energy balance is established as [13, 24]

$$\frac{dT_{fc}}{dt} = \frac{1}{m_{fc} C_{fc}} (H^{in} + H^r - H^{out} - U_{fc} I_{fc} - H_{cv} + H_{cc})$$

(2)

where  $m_{fc}$  and  $C_{fc}$  are the stack's mass and specific heat capacity of SOFC, respectively.  $H^{in}$ ,  $H^r$  and  $H^{out}$  are respectively the input heat flux, the generated heat flux and the output heat flux removed by output gases, which are given in Appendix A. Between the surface of the SOFC stack and the climatic chamber, there are two types of heat flux taken into account, which are the convection heat flux  $H_{cv}$ , and the heat flux provided by the heating and cooling process of the climatic chamber  $H_{cc}$ . They are modeled as

$$H_{cv} = a_1 T_{fc} + a_2$$

$$H_{cc} = K_{cc} R_{cc}$$

where  $a_1$  and  $a_2$  are empirical constants of the convection heat. The power rate of the climatic chamber is denoted as  $R_{cc}$ . And  $K_{cc}$  is the empirical constant for the climatic chamber model.

## 2.3. Problem Formulation

The model of a SOFC system is highly nonlinear, where many parameters in the model cannot be directly determined through experiments. Besides, material properties of a SOFC stack are slowly time-varying during the SOFC operation. To be specific, the theoretical potential  $\Delta U$  is usually considered as 1.2 V. However, this value is not precise in practice and it could be affected by the operation temperature. Moreover, charge transfer constants  $\alpha_{an}$  and  $\alpha_{ca}$  for activation losses show the property of the charge transfer, which can be changed based on the operation condition. Ohmic losses  $U_{ohm}$  have a major impact on the electrochemical model for the practical SOFC, where the reference resistance  $R_0$  is affected by the operation condition. For the model of the thermal balance, it is difficult to determine the empirical constant of the convection heat  $a_1$ . Meanwhile, the coefficient of climatic chamber  $K_{cc}$  is an unknown parameter. Therefore, parameter estimation methods of the nonlinear system identification are required in order to enhance the accuracy of the SOFC model.

In this paper, the following parameters in the SOFC model are chosen as unknown parameters:

$$\Theta_1 = [a_1 \quad K_{cc}]$$

$$\Theta_2 = \left[ \Delta U \quad R_0 \quad \frac{1}{\alpha_{ca}} \quad \frac{1}{\alpha_{an}} \right]$$

Furthermore, the aforementioned mathematical models (1) and (2) can be rewritten as the following nonlinear state-space model:

$$\dot{T}_{fc} = \Phi_1 \Theta_1 + W_1 \quad (3)$$

$$U_{fc} = \Phi_2 \Theta_2 + W_2 \quad (4)$$

where the temperature  $T_{fc}$  is the measurable state and the voltage  $U_{fc}$  represents the system output. Moreover, the computable regressor vectors  $\Phi_1$  and  $\Phi_2$  are expressed as

$$\Phi_1 = \left[ -\frac{T_{fc}}{m_{fc} C_{fc}} \quad \frac{R_{cc}}{m_{fc} C_{fc}} \right]^T$$

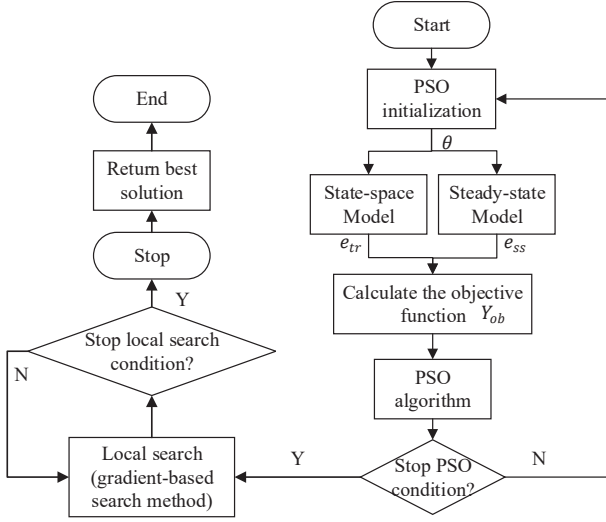


**Figure 2:** Flowchart of the model calibration based on the PSO method and the gradient-based search method.

$$\Phi_2 = \begin{bmatrix} N_{cell} \\ -N_{cell}I_{fc}f_2(T_{fc}) \\ -N_{cell}T_{fc}f_3(I_{fc}) \\ -N_{cell}T_{fc}f_4(I_{fc}) \end{bmatrix}.$$

The known nonlinear functions are  $W_1 = \frac{1}{m_{fc}C_{fc}}(H^{in} + H^r - H^{out} - U_{fc}I_{fc} - a_2)$  and  $W_2 = f_1(T_{fc}) - N_{cell}U_{con}$ .

Hence, this paper aims to investigate offline and online parameter estimation methods to estimate unknown parameters for a SOFC system through measurable temperature  $T_{fc}$ , voltage  $U_{fc}$  and current  $I_{fc}$ . The offline tuning strategy is proposed to calibrate the SOFC model under multiple operation conditions such that the calibrated model is suitable for various operation conditions. To show the time-varying material properties of a SOFC stack, an adaptive optimal parameter estimation method is proposed to estimate unknown parameters online for each operation condition.

### 3. Offline Parameter Estimation Method

In this section, we will present an offline global tuning strategy in order to achieve tuning the SOFC model under different operation conditions.

The complete model of the SOFC system proposed in [25] can be summarized as the nonlinear state-space model, that is

$$\begin{aligned} \dot{x} &= f(x, u, \Theta_1, \Theta_2) \\ y &= h(x, u, \Theta_1, \Theta_2), \end{aligned} \quad (5)$$

where  $x \in \mathbb{R}^{n \times 1}$  denotes as the state vector, where the temperature  $T_{fc}$  is the measurable state.  $u \in \mathbb{R}^{m \times 1}$  represents the input, which is the current  $I_{fc}$  and the input mass flows of hydrogen and air for the SOFC system.  $y \in \mathbb{R}^{r \times 1}$  is the measurable output, where the voltage  $U_{fc}$  is considered as the output for the SOFC system.  $f \in \mathbb{R}^{n \times 1}$  and  $h \in \mathbb{R}^{r \times 1}$

are nonlinear function vectors. Hence, (3) and (4) belong to the state-space model (5).

The state-space model in (5) contains the information of transient and steady-state behaviors. Only regarding to steady-state behavior, the steady-state model is taken into account, where the system can keep the stable condition forever unless an external disturbance applies on the system [22]. In the steady-state condition, the system inputs, states and outputs are at the equilibrium points. Thus, the steady-state model is expressed as:

$$0 = f(x_{eq}, u_{eq}, \Theta_1, \Theta_2) \quad (6)$$

$$y_{eq} = h(x_{eq}, u_{eq}, \Theta_1, \Theta_2), \quad (7)$$

where  $x_{eq}$ ,  $u_{eq}$  and  $y_{eq}$  represent the state, the input and the output at the equilibrium points, respectively. It is worthy noting that the system includes infinite equilibrium points, where equilibrium points  $x_{eq}$  and  $u_{eq}$  are directly determined by (6). Then the output equilibrium points  $y_{eq}$  in (7) are computed through the obtained equilibrium points  $x_{eq}$  and  $u_{eq}$ .

**Remark 1.** For a fuel cell, the polarization curve illustrates the steady-state voltage at a given current. Consequently, the steady-state model of (7) is the model to interpret the polarization curve of a fuel cell. Moreover, the electrochemical impedance spectroscopy (EIS) technique [1] is a common diagnostic testing method for a fuel cell, which can be used to determine the equivalent circuit of the fuel cell. For each EIS test, the impedance spectra of the fuel cell is recorded when the fuel cell stack reaches to the steady-state voltage by a given current. Thus, the EIS test provides the information from the equilibrium point, which also can be interpreted by the steady-state model of (7). In this paper, we only focus on the polarization curve of a SOFC to determine the steady-state model of (7).

The state-space model (5) and the steady-state model (6), (7) explicitly depend on the system parameters  $\Theta_1$  and  $\Theta_2$ . Thus, output errors for the state-space model  $e_{tr}$  and the steady-state model  $e_{ss}$  are calculated as:

$$\begin{aligned} e_{tr}(\Theta_1, \Theta_2, t) &= \|U_e(t) - U_{fc}(\Theta_2, t)\|^2 + \|T_e(t) - T_{fc}(\Theta_1, t)\|^2 \\ e_{ss}(\Theta_2, i) &= \|U_a(i) - U_{fc,eq}(\Theta_2, i)\|^2 \end{aligned}$$

where  $U_e$  and  $T_e$  are the experimental data of voltage and temperature, respectively;  $U_a$  denotes the value of the steady-state behavior for the experimental voltage data.  $U_{fc,eq}$  is the output equilibrium points of the voltage.

In order to achieve calibrating the state-space model (5) and the steady-state model (6), (7) simultaneously, an objective function is defined based on the mean-square error:

$$J(\Theta_1, \Theta_2) = \alpha_0 \sum_{t=0}^{i=kT_s} e_{tr}(\Theta_1, \Theta_2, t) + (1 - \alpha_0) \sum_{i=1}^{N_e} e_{ss}(\Theta_2, i)$$

where  $N_e$  denotes the number of experimental steady-state value  $U_{ave}$ ;  $T_s$  is the sampling time and  $k$  is the sampling

period, which both depend on the experiment;  $\alpha_0$  represented as a weight constant to be manually set, which is  $0 \leq \alpha_0 \leq 1$ . The weight constant  $\alpha_0$  is used to make a trade-off between calibrating the state-space model (5) and the steady-state model (6), (7). When the experimental data contains more information of the steady-state behavior, the weight constant  $\alpha_0$  can be set as a small value. Especially, only the steady-state model is to be calibrated when the weight constant is set as  $\alpha_0 = 0$ .

Thus, the problem of the model tuning can be summarized as

$$\begin{aligned} & \min_{\Theta_1, \Theta_2} J(\Theta_1, \Theta_2) \\ \text{s.t. } & \Theta_{1,min} \leq \Theta_1 \leq \Theta_{1,max}, \\ & \Theta_{2,min} \leq \Theta_2 \leq \Theta_{2,max} \end{aligned} \quad (8)$$

where  $\Theta_{1,min}$  and  $\Theta_{2,min}$  are the minimum values of  $\Theta_1$  and  $\Theta_2$ , respectively. The maximum values of  $\Theta_1$  and  $\Theta_2$  are respectively denoted as  $\Theta_{1,max}$  and  $\Theta_{2,max}$ . They can be set based on their physical properties and empirical value.

Since the cost function (8) may not be a convex problem, the widely used PSO method with the classic gradient-based search method is used to minimize the objective function  $J$  for each operation condition. The flowchart of the model calibration for each operation condition is shown in Figure 2. To be specific, the mathematical model of the fuel cell system is first built by using MATLAB/Simulink. Then, a mapping of potential parameter  $\Theta_1$  and  $\Theta_2$  given by PSO are used for the state-space model (5) and the steady-state model (6), (7) to obtain the tuning errors  $e_{tr}$  and  $e_{ss}$ . To get equilibrium points for computing  $e_{ss}$ , it is not trivial due to the highly nonlinear property of the steady-state model (6), (7). We can numerically solve the steady-state model of (6) and (7) through using the given value for the equilibrium points of the input  $u_{eq}$  and the stack temperature  $T_{fc,eq}$ . Meanwhile, we can set initial values for each state in order to avoid divergent results during the numerical solving procedure. Consequently, the 'findop' MATLAB command has been used to compute equilibrium points. Furthermore, the PSO will minimize the objective function  $J$  in order to achieve the global search. When the maximum number of PSO iteration is satisfied, the tuning parameters  $\Theta_1$  and  $\Theta_2$  are near optimum points. Additionally, the solution from PSO is set as initial points for the classic gradient-based search method. The gradient-based search method will be used to achieve the local search and to obtain more precise solution. The merits of the PSO method with the gradient-based search method are its faster convergence and more efficient response since the number of potential parameters for PSO can be reduced and the gradient-based search method has a good performance for the local search. Finally, the PSO method with the gradient-based search method is implemented by the MATLAB command 'particleswarm' and 'fmincon'.

After using the PSO method with the classic gradient-based search method for each operation condition, the solution of  $\Theta_1$  and  $\Theta_2$  is different among multiply operation

conditions. In order to obtain a group of the solution for  $\Theta_1$  and  $\Theta_2$  under different operation conditions, an offline tuning strategy for a SOFC system is proposed. Specifically, there are three steps to achieve minimize the objective function  $J$  under various operation conditions.

1. The PSO method with the gradient-based search method in Figure 2 is used to tune the state-space model (5) and the steady-state model (6), (7) for each operation condition.
2. The sensitive parameters with respect to the operation condition are expanded into the polynomial equations.
3. The whole unknown parameters including coefficients in the polynomial equations are determined by using the PSO method with the gradient-based search method again under whole operation conditions.

Finally, the mathematical model of fuel cell systems for different operation conditions can be calibrated offline based on the proposed tuning strategy.

#### 4. Online Parameter Estimation Method

The mathematical model of a SOFC system for multiple operation conditions can be obtained offline by the proposed tuning strategy. However, material properties of a SOFC stack are slowly changing during the operation time. In order to show the time-varying performance of unknown parameters, an online parameter estimation method is presented in this section for each operation condition. Moreover, the following assumptions for the proposed online parameter estimation method are first provided as:

**Assumption 1.** The unknown parameters  $\Theta_1, \Theta_2$  are slowly time-varying and their derivatives are bounded such that  $\|\dot{\Theta}_1\| \leq v_1$  and  $\|\dot{\Theta}_2\| \leq v_2$  hold for positive constants  $v > v_1 > 0$  and  $v > v_2 > 0$ .

**Remark 2.** For SOFC, the unknown parameters are changing slowly such that Assumption 1 can be trivially fulfilled. Besides, the upper bounds  $v, v_1$  and  $v_2$  are not needed to known, which are used for the following analysis.

For SOFC, it is trivial to measure the SOFC stack temperature and voltage in practice. In order to avoid requiring the information of temperature derivative  $\dot{T}_{fc}$  in (3), the following filtered variables are given as:

$$\begin{cases} \kappa \dot{T}_{fc,f} + T_{fc,f} = T_{fc}, & T_{fc}(0) = 0 \\ \kappa \dot{\Phi}_{1,f} + \Phi_{1,f} = \Phi_1, & \Phi_1(0) = 0 \\ \kappa \dot{W}_{1,f} + W_{1,f} = W_1, & W_1(0) = 0 \end{cases} \quad (9)$$

where  $\kappa$  is a tuning constant. For the practical SOFC, the SOFC temperature  $T_{fc}$ , voltage  $U_{fc}$  and current  $I_{fc}$  are bounded and measurable. Meanwhile, parameters in  $\Phi_1$  are considered as known constants. Thus, we can derive that the vector  $\Phi_1$  is bounded. Furthermore, the filtered variable  $\Phi_{1,f}$  is bounded such that the fact  $\|\Phi_{1,f}\| \leq \gamma$  fulfills for a positive constant  $\gamma > 0$ .

To show the effectiveness of the defined variables in (9), the thermal energy balance of SOFC in (3) is filtered by a low-pass filter  $1/(\kappa s + 1)$ . Consequently, we can get

$$\frac{s}{\kappa s + 1} \{T_{fc}\} = \frac{1}{\kappa s + 1} \{\Phi_1 \Theta_1\} + \frac{1}{\kappa s + 1} \{W_1\}. \quad (10)$$

Compared (10) with (9), we can further derive the following equation based on the Swapping Lemma [8].

$$\begin{aligned} \dot{T}_{fc,f} &= \frac{T_{fc} - T_{fc,f}}{\kappa} = \Phi_{1,f} \Theta_1 - \frac{\kappa}{\kappa s + 1} \{\Phi_{1,f} \dot{\Theta}_1\} + W_{1,fc} \\ &= \Phi_{1,f} \Theta_1 + W_{1,fc} + d \end{aligned} \quad (11)$$

where the bounded disturbance denotes as  $d = -\kappa/(\kappa s + 1) \{\Phi_{1,f} \dot{\Theta}_1\}$ , which fulfills  $\|d\| \leq \zeta_d$  for a constant  $\zeta_d > 0$ . Moreover, it can be neglected that the initial value passes through the low-pass filter, which will be exponentially vanishing.

**Lemma 1.** *For the disturbance  $d = 0$  satisfied, the auxiliary variable is expressed as*

$$z = \frac{T_{fc} - T_{fc,f}}{\kappa} - \Phi_{1,f} \Theta_1 - W_{1,fc}, \quad (12)$$

which is uniformly ultimately bounded with the property of exponentially converging to a compact set around zero such that the fact

$$\lim_{\kappa \rightarrow 0} \{ \lim_{t \rightarrow \infty} \{(T_{fc} - T_{fc,f})/\kappa - \Phi_{1,f} \Theta_1 - W_{1,fc}\} \} = 0 \quad (13)$$

holds. Consequently, the invariant manifold  $(T_{fc} - T_{fc,f})/\kappa - \Phi_{1,f} \Theta_1 - W_{1,fc} = 0$  is obtained for  $\kappa > 0$  and  $d = 0$ .

**PROOF.** To proof the boundedness of the auxiliary variable  $z$ , we first take the differential of (12), that is

$$\dot{z} = -(z + \kappa \Phi_{1,f} \dot{\Theta}_1)/\kappa.$$

Then we choose  $V_z = z^T z / 2$  as Lyapunov function. Its derivative is

$$\begin{aligned} \dot{V}_z &= -\frac{1}{\kappa} z^T \dot{z} - z^T \Phi_{1,f} \dot{\Theta}_1 \\ &\leq -\frac{1}{\kappa} \|z\|^2 + \frac{1}{2\kappa} \|z\|^2 + \frac{\kappa}{2} \|\Phi_{1,f} \dot{\Theta}_1\|^2 \\ &\leq -\frac{1}{\kappa} V_z + \frac{\kappa}{2} \gamma^2 v_1^2. \end{aligned}$$

Furthermore, we can get that  $V_z(t) \leq e^{-t/\kappa} V_z(0) + \kappa^2 \gamma^2 v_1^2 / 2$ . Thus, the auxiliary variable  $z$  is uniformly ultimately bounded.

Subsequently, we can derive that  $\|z\| = \sqrt{2V_z} \leq \sqrt{z^2(0)e^{-t/\kappa} + \kappa^2 \gamma^2 v_1^2}$  such that we can conclude that the auxiliary variable  $z$  will exponentially converge to a small compact set. This compact set is determined by the constant  $\kappa$  and the upper bounds of  $\Phi_{1,f}$  and  $\dot{\Theta}_1$ . Besides, we can get the fact  $\lim_{t \rightarrow \infty} z = \kappa \gamma v_1$  for  $\kappa > 0$  and  $d = 0$ . Furthermore, we can derive that the auxiliary variable  $z$  can reduce to zero

(i.e.,  $\lim_{\kappa \rightarrow 0} \lim_{t \rightarrow \infty} z = 0$ ) when the constant  $\kappa$  is a small value or the unknown parameter  $\Theta_1$  is constant (i.e.,  $\dot{\Theta}_1 = 0$ ). Therefore, we can conclude that  $z = 0$  is an invariant manifold for  $\kappa > 0$  [3].

It is worth mentioning that the invariant manifold  $z$  in (12) is independent of the temperature derivative  $\dot{T}_{fc}$ . Based on this fact, the model of SOFC can be rewritten as the following based on (4) and (11).

$$Y = \Phi \Theta + D_d \quad (14)$$

where  $Y = [(T_{fc} - T_{fc,f})/\kappa - W_{1,f} \quad U_{fc} - W_2]^T$  is the known output.  $\Theta = [\Theta_1 \quad \Theta_2]$  is the unknown parameter to be estimated. Based on Assumption 1, the parameter derivative is bounded such that the fact  $\|\dot{\Theta}\| \leq v$  holds for a positive constant  $v > 0$ .  $\Phi = \text{diag}\{\Phi_{1,f} \quad \Phi_2\}$  is the calculable regressor matrix, which is bounded (i.e.,  $\|\Phi\| \leq \gamma_1, \forall \gamma_1 > 0$ ).  $\text{diag}\{\cdot\}$  denotes as the diagonal matrix. Moreover,  $D_d = [d \quad 0]^T$  is considered as the bounded disturbance vector, that is  $\|D_d\| \leq \zeta_d$ .

In order to derive the adaptive law, the filtered matrices are defined as

$$\begin{cases} \dot{P}_1 = -\ell P_1 + \Phi^T \Phi / m_1^2, & P_1(0) = 0 \\ \dot{Q}_1 = -\ell Q_1 + \Phi^T Y / m_1^2, & Q_1(0) = 0 \\ \dot{H}_1 = -\ell H_1 + [\Phi^T (Y - \Phi \hat{\Theta})] / m_1^2 - P_1 \dot{\hat{\Theta}}, & H_1(0) = 0 \end{cases} \quad (15)$$

where  $\ell > 0$  is a constant to ensure that the matrix  $P_1$  and vectors  $Q_1, H_1$  are bounded. The normalizing signal is  $m_1^2 = 1 + \|\Phi^T \Phi\|$ .  $\hat{\Theta}$  is the estimated parameter.

Then, we can derive the following matrix, which is related to the estimated parameter  $\hat{\Theta}$ .

$$\begin{cases} H_1 = Q_1 - P_1 \hat{\Theta} \\ h = (\Phi^T \Phi \hat{\Theta} - \Phi^T Y) / m_1^2 \end{cases} \quad (16)$$

**Lemma 2.** *The defined matrix in (16) can be further derived the following fact, that is:*

$$H_1 = P_1 \tilde{\Theta} - D_1 \quad (17)$$

$$h = -(\Phi^T \Phi \tilde{\Theta} + \Phi^T D_d) / m_1^2 \quad (18)$$

where the estimated error is denoted as  $\tilde{\Theta} = \Theta - \hat{\Theta}$ .  $D_1 = \int_0^t e^{-\ell(t-\tau)} (\Phi^T(\tau) D_d(\tau) / m_1^2(\tau) - P_1(\tau) \dot{\hat{\Theta}}(\tau)) d\tau$  is considered as a bounded residual disturbance, that is  $\|D_1\| \leq \zeta_1$  for a constant  $\zeta_1 > 0$ . Moreover,  $\Phi^T D_d / m_1^2$  is also a bound disturbance, that is  $\Phi^T D_d / m_1^2 \leq \gamma_1^2 / (2\kappa m_1^2) + k \zeta_d^2 / (2m_1^2) \leq \zeta_2$  for constants  $k > 0$  and  $\zeta_2 > 0$ .

**PROOF.** First, we integrate (15) and further get

$$\begin{cases} P_1 = \int_0^t e^{-\ell(t-\tau)} \Phi^T(\tau) \Phi(\tau) / m_1^2(\tau) d\tau \\ Q_1 = \int_0^t e^{-\ell(t-\tau)} \Phi^T(\tau) Y(\tau) / m_1^2(\tau) d\tau. \end{cases} \quad (19)$$

From (14), we can derive that  $Y - \Phi\hat{\Theta} = \Phi\tilde{\Theta} + D_d$ . By multiplying  $e^{\ell t}$  into (15) and substituting (19), we get

$$\begin{aligned} & e^{\ell t}\dot{H}_1 + \ell e^{\ell t}H_1 \\ &= e^{\ell t}\frac{\Phi^T\Phi}{m_1^2}\tilde{\Theta} + e^{\ell t}\frac{\Phi^T D_d}{m_1^2} - e^{\ell t}P_1\dot{\Theta} + e^{\ell t}P_1\dot{\Theta} \\ &= e^{\ell t}\frac{\Phi^T\Phi}{m_1^2}\tilde{\Theta} + \left(\int_0^t e^{\ell\tau}\frac{\Phi^T(\tau)\Phi(\tau)}{m_1^2(\tau)}d\tau\right)\dot{\Theta} \\ & \quad + e^{\ell t}\left(\frac{\Phi^T D_d}{m_1^2} - P_1\dot{\Theta}\right). \end{aligned} \quad (20)$$

Then we can further get

$$\begin{aligned} \frac{d}{dt}\{e^{\ell t}H_1\} &= \frac{d}{dt}\left[\left(\int_0^t e^{\ell\tau}\frac{\Phi^T(\tau)\Phi(\tau)}{m_1^2(\tau)}d\tau\right)\dot{\Theta}\right] \\ & \quad + e^{\ell t}\left(\frac{\Phi^T D_d}{m_1^2} - P_1\dot{\Theta}\right). \end{aligned} \quad (21)$$

By integrating it, we get

$$\begin{aligned} H_1 &= \left(\int_0^t e^{-\ell(t-\tau)}\frac{\Phi^T(\tau)\Phi(\tau)}{m_1^2(\tau)}d\tau\right)\tilde{\Theta} \\ & \quad + \int_0^t e^{-\ell(t-\tau)}\left(\frac{\Phi^T(\tau)D_d(\tau)}{m_1^2(\tau)} - P_1(\tau)\dot{\Theta}(\tau)\right)d\tau \end{aligned} \quad (22)$$

Hence, (17) can be obtained. Then the fact (18) can be proved by combining (14) with (16).

From Lemma 2, the matrix  $H_1$  and the vector  $h$  contain the estimation error  $\tilde{\Theta}$ . In the following, we adopt the idea of optimization to establish a cost function and minimize the estimation error  $\tilde{\Theta}$ . Moreover, a time-varying gain can be derived to improve the performance of the matrix  $H_1$ , the vector  $h$  and further achieve parameter estimation.

In order to contain the information of the matrix  $H_1$  and the vector  $h$ , auxiliary matrices are first defined as

$$\begin{cases} P = P_1 + \beta\Phi^T\Phi/m_1^2 \\ Q = Q_1 + \beta\Phi^T Y/m_1^2 \end{cases} \quad (23)$$

where  $\beta > 0$  is a constant coefficient. The matrices  $P$  and  $Q$  are bounded by  $\|P\| \leq \mu_1$  for a constant  $\mu_1 > 0$ .

Furthermore, the cost function for the optimization is expressed as

$$\begin{aligned} J(\hat{\Theta}, t) &= \frac{1}{2}\int_0^t e^{-l(t-\tau)}\frac{[Q(\tau) - P(\tau)\hat{\Theta}(t)]^T[Q(\tau) - P(\tau)\hat{\Theta}(t)]}{m^2(\tau)}d\tau \\ & \quad + \frac{1}{2}e^{-lt}[\hat{\Theta}(t) - \hat{\Theta}(0)]^T S_0[\hat{\Theta}(t) - \hat{\Theta}(0)] \end{aligned} \quad (24)$$

where the normalizing signal is denoted as  $m^2 = 1 + \|P^T P\|$ .  $S_0 = S_0^T > 0$  is the constant weight matrix.  $l$  is the forgetting constant, which used to exponentially decrease the effect of initial value  $\hat{\Theta}(0)$ .

Since the convexity of the cost function  $J_1(\hat{\Theta}, t)$  with respect to  $\hat{\Theta}$ , the optimization problem is expressed as

$$\begin{aligned} \min \quad & \frac{\partial J(\hat{\Theta}, t)}{\partial \hat{\Theta}} = 0 \\ \text{s.t.} \quad & t > 0. \end{aligned} \quad (25)$$

Subsequently, we can derive that

$$\begin{aligned} \frac{\partial J(\hat{\Theta}, t)}{\partial \hat{\Theta}} &= e^{-lt}S_0[\hat{\Theta}(t) - \hat{\Theta}(0)] \\ & \quad - \int_0^t e^{-l(t-\tau)}\frac{P^T(\tau)Q(\tau) - P^T(\tau)P(\tau)\hat{\Theta}(t)}{m^2(\tau)}d\tau = 0. \end{aligned} \quad (26)$$

Then, (26) can be rewritten as

$$\hat{\Theta} = \Gamma S \quad (27)$$

where the inverse of time-varying gain is expressed as

$$\Gamma^{-1} = \int_0^t e^{-l(t-\tau)}\frac{P^T(\tau)P(\tau)}{m^2(\tau)}d\tau + e^{-lt}S_0. \quad (28)$$

And the matrix  $S$  is expressed as

$$S = \int_0^t e^{-l(t-\tau)}\frac{P^T(\tau)Q(\tau)}{m^2(\tau)}d\tau + e^{-lt}S_0\hat{\Theta}(0) \quad (29)$$

However, it is nontrivial to compute (27) with (28) and (29) for estimating parameter online. In order to address this problem, we first differentiate (28), that is:

$$\begin{aligned} \frac{d}{dt}\{\Gamma^{-1}\} &= -l\int_0^t e^{-l(t-\tau)}\frac{P^T(\tau)P(\tau)}{m^2(\tau)}d\tau \\ & \quad - le^{-lt}S_0 + \frac{P^T P}{m^2} \\ &= -l\Gamma^{-1} + \frac{P^T P}{m^2}. \end{aligned} \quad (30)$$

Then, we consider the following equality [8], that is

$$\frac{d}{dt}\{\Gamma\Gamma^{-1}\} = \dot{\Gamma}\Gamma^{-1} + \Gamma\frac{d}{dt}\{\Gamma^{-1}\} = 0. \quad (31)$$

Based on (30) and (31), we can derive that

$$\dot{\Gamma} = l\Gamma - \Gamma\frac{P^T P}{m^2}\Gamma, \quad \Gamma^{-1}(0) = S_0 > 0 \quad (32)$$

Following the same procedure for the matrix  $S$ , we get

$$\dot{S} = -lS + \frac{P^T Q}{m^2} \quad (33)$$

Based on (23) the adaptive law is designed as

$$\begin{aligned} \dot{\hat{\Theta}} &= \dot{\Gamma}S + \Gamma\dot{S} \\ &= (l\Gamma - \Gamma\frac{P^T P}{m^2}\Gamma)S + \Gamma(-lS + \frac{P^T Q}{m^2}) \\ &= \Gamma\frac{P^T(Q - P\hat{\Theta})}{m^2} = \Gamma\frac{P^T(H_1 - \beta h)}{m^2} \end{aligned} \quad (34)$$

Before we show the convergence of the adaptive law (34), the regressor matrix  $\Phi$  fulfilling the persistent excitation (PE) condition needs to be defined and analyzed. Besides, the boundedness of time-varying gain  $\Gamma$  is required to analyze.

**Lemma 3.** [15] *The regressor matrix  $\Phi$  fulfills the PE condition such that  $\exists T_1 > 0$ ,  $\delta_1 > 0$ ,  $\int_t^{t+T_1} \Phi(\tau)^T \Phi(\tau) d\tau \geq \delta_1 I$ ,  $\forall t \geq 0$ . Moreover, the positive definite matrix  $P_1$  in (15) can be derived, such that the minimum eigenvalue  $\lambda_{\min}\{P_1\}$  is large than zero (i.e.,  $\lambda_{\min}\{P_1\} > \epsilon_1 > 0$ ,  $\forall \epsilon_1 > 0$ ).*

**Lemma 4.** *Based on the fact that the regressor matrix  $\Phi$  fulfills the PE condition, the time-varying gain  $\Gamma$  satisfies that*

$$\underline{\omega} I \leq \Gamma \leq \overline{\omega} I \quad (35)$$

where the lower bound is  $\underline{\omega} = 1/(\lambda_{\min}\{S_0\} + 1/l) > 0$  and the upper bound is  $\overline{\omega} = e^{lT_2} m^2 / \epsilon_1^2 > 0$ .

PROOF. Based on the facts  $P^T P / m^2 \leq I$  and  $\int_0^t e^{-l(t-\tau)} d\tau \leq 1/l$ , (28) can be derived that

$$\Gamma^{-1} \leq I \int_0^t e^{-l(t-\tau)} d\tau + S_0 \leq I/l + S_0 \quad (36)$$

From the PE condition illustrated in Lemma 3, (28) can be obtained that for  $t > T_2 > 0$ ,

$$\begin{aligned} \Gamma^{-1} &\geq \int_0^t e^{-l(t-\tau)} \frac{P^T(\tau)P(\tau)}{m^2(\tau)} d\tau \\ &\geq \int_{t-T_2}^t e^{-l(t-\tau)} \frac{P^T(\tau)P(\tau)}{m^2(\tau)} d\tau \geq \frac{\epsilon_1^2}{m^2} e^{-lT_2} I. \end{aligned} \quad (37)$$

Finally, (35) is verified.

In the following, the convergence of the proposed adaptive law (34) is provided.

**Theorem 5.** *Consider system (3) and (4) with Assumption 1, the adaptive law (29) with the filter operation (9) and auxiliary variable (15) is used. Moreover, the system satisfies the PE condition defined in Lemma 3, then the estimation error  $\tilde{\Theta} = \Theta - \hat{\Theta}$  will exponentially converge to a compact set around zero.*

PROOF. We choose  $V = \tilde{\Theta}^T \Gamma^{-1} \tilde{\Theta} / 2$  as the Lyapunov function. Then, its derivative is expressed as

$$\begin{aligned} \dot{V} &= \tilde{\Theta}^T \Gamma^{-1} \dot{\tilde{\Theta}} + \frac{1}{2} \dot{\tilde{\Theta}}^T \Gamma^{-1} \tilde{\Theta} \\ &= \tilde{\Theta}^T \Gamma^{-1} \dot{\tilde{\Theta}} - \frac{l}{2} \tilde{\Theta}^T \Gamma^{-1} \tilde{\Theta} - \frac{1}{2} \tilde{\Theta}^T \frac{P^T P}{m^2} \tilde{\Theta} \\ &\quad + \tilde{\Theta}^T \frac{P^T D_1}{m^2} - \beta \tilde{\Theta}^T \frac{P^T \Phi^T D_d}{m^2 m_1^2} \end{aligned} \quad (38)$$

Then we apply the Young's inequality with a constant  $k_1 > 0$ . We can get

$$\begin{aligned} \dot{V} &\leq -\left(\frac{\epsilon_1^2}{m^2} - \frac{3}{2k_1} + \frac{l}{\overline{\omega}}\right) \|\tilde{\Theta}\|^2 + \frac{k_1 v^2}{2\overline{\omega}^2} + \frac{k_1 \mu_1^2 \zeta_1^2}{2m^2} + \frac{k_1 \beta^2 \mu_1^2 \zeta_2^2}{2m^2} \\ &\leq -aV + b \end{aligned} \quad (39)$$

**Table 1**

Search range of unknown parameters in the SOFC model for each operation condition

Parameter	$\Delta U$	$R_0$	$\alpha_{ca}$	$\alpha_{an}$	$a_1$	$K_{cc}$
Lower	1	0.5	0.2	0.2	0.01	1
Upper	1.2	1.5	10	10	15	250

**Table 2**

Tuning results for unknown parameters in the SOFC model for each operation condition

Parameter	$\Delta U$	$R_0$	$\alpha_{ca}$	$\alpha_{an}$	$a_1$	$K_{cc}$
750°C	1.069	1.331	10.000	2.474	14.851	8.116
790°C	1.057	1.203	10.000	0.608	11.553	250.000

where  $a = \epsilon_1^2 / m^2 - 3/(2k_1) + l/\overline{\omega}$  and  $b = k_1 v^2 / 2\overline{\omega}^2 + k_1 \mu_1^2 \zeta_1^2 / 2m^2 + k_1 \beta^2 \mu_1^2 \zeta_2^2 / 2m^2$  are positive constants for  $k_1 \geq 3/(2\epsilon_1^2 / m^2 + 2/\overline{\omega})$ . The solution of (39) is  $V \leq e^{-at} V(0) + b/a$ . Then we can further derive that  $\|\tilde{\Theta}\|^2 \leq \sqrt{2V\overline{\omega}} \leq \sqrt{\|\tilde{\Theta}(0)\|^2 \overline{\omega}^2 e^{-at} + 2b\overline{\omega}/a}$ . Hence, the estimation error  $\tilde{\Theta}$  will exponentially converge to a compact set around zero.

## 5. Practical Model Tuning and Validation

In this part, the experiment is conducted on the practical SOFC test bench (as shown in Figure 1) for two operation conditions. The target temperature of SOFC for two operation condition is set as 750°C and 790°C. The sweeping current range is set from 0 A to 13 A. The mass flows of hydrogen and oxygen are set as 4.88 slpm and 15 slpm, respectively. The experimental data of the system input for SOFC is shown in Figure 3.

### 5.1. Offline Model Tuning Results

Based on the proposed tuning strategy, the PSO search range setup for unknown parameters under two operation conditions is provided in Table 1. Subsequently, by using the PSO method with the gradient-based search method for each case, tuning results are shown in Table 2. Moreover, the following parameters are the chosen sensitive parameters, which are expanded into the polynomial equations with respect to the stack temperature  $T_{fc}$ :

$$\begin{aligned} \Delta U &= \Delta U_{01} + \Delta U_{02}(T_{fc} - T_0) \\ R_0 &= R_{01} + R_{02}(T_{fc} - T_0) \\ \alpha_{ca} &= \alpha_{ca1} + \alpha_{ca2}(T_{fc} - T_0) \\ \alpha_{an} &= \alpha_{an1} + \alpha_{an2}(T_{fc} - T_0) \end{aligned} \quad (40)$$

where the reference temperature is set as  $T_0 = 700^\circ\text{C}$ .

The SOFC model with (40) is considered as the global model to be calibrated. Table 3 shows the PSO search range of unknown parameters in the SOFC global model. To make the value of polynomial equations fulfill the search range in

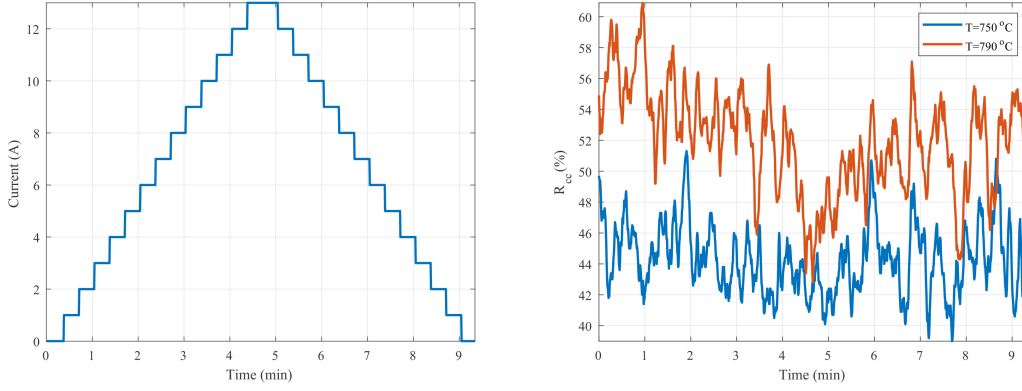


**Figure 3:** The experimental data of the input for SOFC (current  $I_{fc}$  and power rate of the climatic chamber  $R_{cc}$ ).

**Table 3**

Search range of the unknown parameters in the SOFC model for whole operation conditions (750°C and 790°C)

Parameter	$\Delta U_{01}$	$\Delta U_{02}$	$R_{01}$	$R_{02}$	$\alpha_{ca1}$
Lower	1	$-8.5 \times 10^{-4}$	0.5	$-4.7 \times 10^{-4}$	0.2
Upper	1.2	$8.5 \times 10^{-4}$	1.5	$4.7 \times 10^{-4}$	10
Parameter	$\alpha_{ca2}$	$\alpha_{an1}$	$\alpha_{an2}$	$a_1$	$K_{cc}$
Lower	$-1.9 \times 10^{-4}$	0.2	$-1.9 \times 10^{-4}$	1	1
Upper	$1.9 \times 10^{-4}$	10	$1.9 \times 10^{-4}$	15	250

**Table 4**

Tuning results for the unknown parameters in the SOFC model for whole operation conditions (750°C and 790°C)

Parameter	$\Delta U_{01}$	$\Delta U_{02}$	$R_{01}$	$R_{02}$	$\alpha_{ca1}$
Value	1.0548	$1.1008 \times 10^{-4}$	1.2566	$-4.7 \times 10^{-4}$	0.2095
Parameter	$\alpha_{ca2}$	$\alpha_{an1}$	$\alpha_{an2}$	$a_1$	$K_{cc}$
Value	$-1.9 \times 10^{-4}$	4.6732	$-1.9 \times 10^{-4}$	14.9905	78.5876

Table 1, the objective function is redefined as follows:

$$J_1 = \begin{cases} J, & \text{if } 1 \leq \Delta U \leq 1.2, \\ & \text{and } 0.5 \leq R_0 \leq 1.5, \\ & \text{and } 0.2 \leq \alpha_{ca} \leq 10, \\ & \text{and } 0.2 \leq \alpha_{an} \leq 10. \\ J + 10^{20}, & \text{otherwise.} \end{cases} \quad (41)$$

Furthermore, the tuning results for the SOFC global model is shown in Table 4 by using the PSO method with the gradient-based search method.

In order to show the calibrated model performance, the comparative results among the model simulation results, the global model simulation results and the experimental data are depicted from Figure 4 to Figure 6. It is shown that the transient behaviors of temperature and voltage from the calibrate model (Figure 4, Figure 5) are similar to the experimental data. Moreover, the global model with one group of tuning parameters in Table 4 can provide similar

performance, compared with the model with two groups of tuning parameters in Table 2. Therefore, it is illustrated that the global tuning strategy is effective to calibrate the SOFC model for various operation conditions. However, there are some discrepancy between simulation results and experimental data. Due to these errors, the steady-state model cannot provide accurate value of the voltage (Figure 6), especially for the case that the current is larger than 6 A.

## 5.2. Online Model Tuning Results

The proposed parameter estimation method will be conducted on the SOFC model by using the same experimental data for each operation condition. The learning parameters in the proposed method (34) are set as  $\kappa = 9 \times 10^{-3}$ ,  $\ell = 70$ , and  $l = 100$ ,  $\beta = 0.05$ . The initial values of the estimated parameters are set as  $\hat{\Theta}_1(0) = [5 \ 100]$ ,  $\hat{\Theta}_2(0) = [1 \ 1 \ 1 \ 1]$ . The sampling time is  $1 \times 10^{-3}$ . The computation time required by the proposed adaptive method at each time step is around  $1.3 \times 10^{-4}$  s.

Figure 7 and Figure 8 illustrates the result profiles of the estimated parameters by using the proposed method (34). It is shown that the estimated parameters are slowly time-varying. In order to verify the estimation results, the temperature and the voltage of the SOFC system are computed by substituting the estimated results and compared with the experimental data. The comparative results are shown in Figure 9. It is shown that the model with estimation results of the proposed method (34) can provide a good performance. Since the offline tuning strategy obtains a constant value of the parameter for the whole experimental data, the unavoidable variations in the system may not be captured. Hence, the proposed adaptive estimation method can obtain a superior performance. However, the proposed adaptive estimation method can only calibrate the model for each operation condition such that it cannot provide a global model. Therefore, the offline global tuning strategy based on the PSO method and the gradient-based search method can be used to tune the SOFC model under variable operation conditions. The proposed adaptive estimation method can

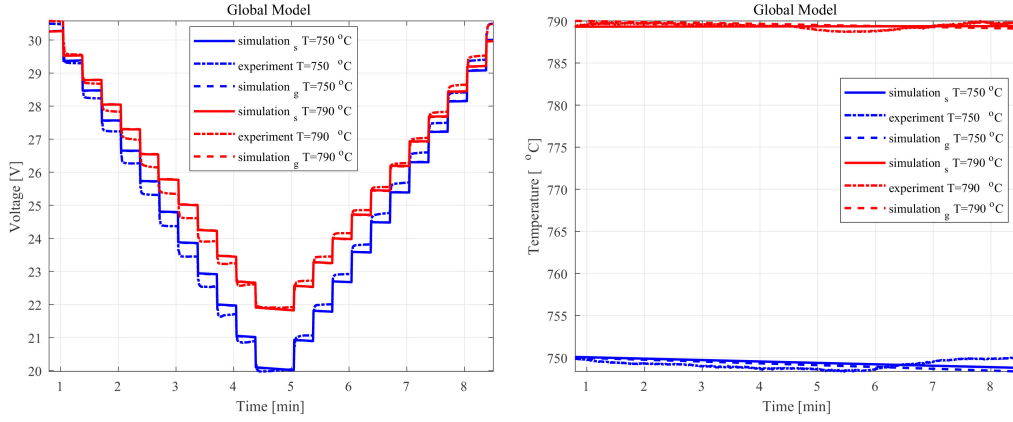


Figure 4: The tuning transient profiles of the SOFC stack voltage and temperature at  $T = 750^{\circ}\text{C}$  and  $T = 790^{\circ}\text{C}$ .

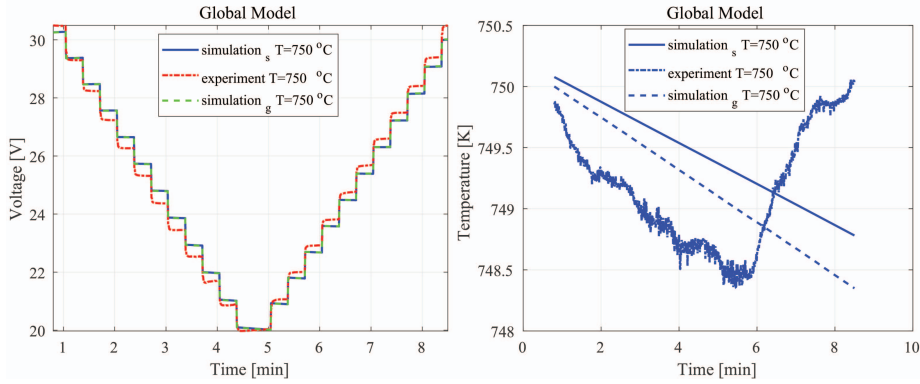


Figure 5: The zoom-in tuning transient profiles of the SOFC stack voltage and temperature at  $T = 750^{\circ}\text{C}$ .

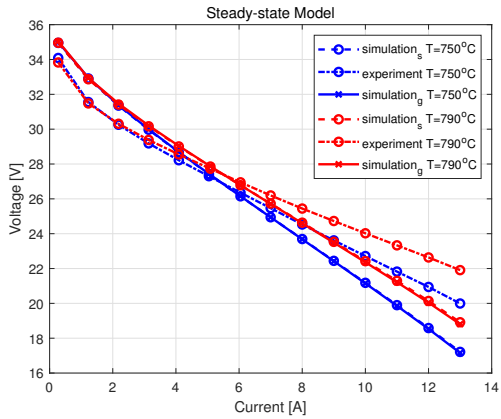


Figure 6: The tuning equilibrium points of the SOFC stack voltage ( $U_{fc}$ ) by using parameter values in Table 4.

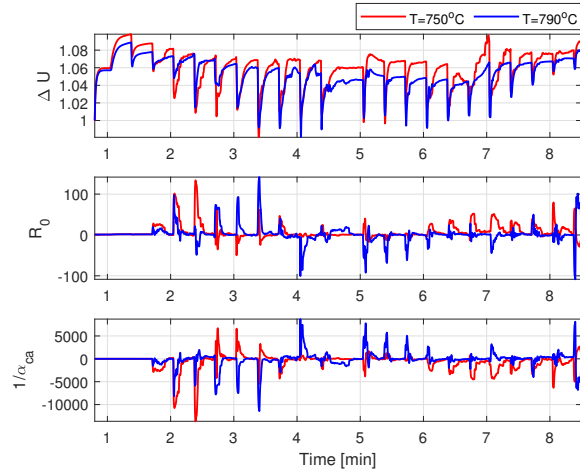


Figure 7: The estimation results by using the proposed adaptive method (34).

be used to estimate the time-varying parameters for each operation conditions.

## 6. Conclusion

In this paper, an offline global tuning strategy and an online parameter estimation method for a SOFC system are

investigated to calibrate the mathematical model. The offline global tuning strategy is developed in order to tuning the model under various operation conditions. First, the PSO method with gradient-based search method is applied to tuning the state-space model and the steady-state model for each operation condition. Then the sensitive parameters are

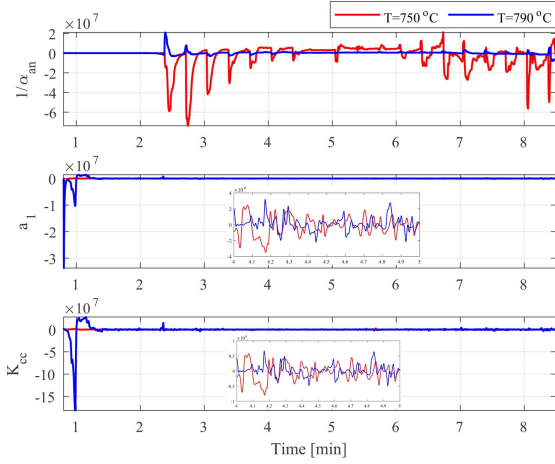


**Figure 8:** The estimation results by using the proposed adaptive method (34).

expanded to the polynomial equations to guarantee global fitting. Moreover, the global model including coefficients in the polynomial equations are determined by using the PSO method with gradient-based search method for whole operation conditions. For online parameter estimation method, an adaptive optimal learning law is proposed to minimize a cost function with the information of the estimation error. The estimation error is extracted through several low-pass filters and simple algebraic calculation. Finally, the proposed tuning strategy and adaptive estimation method are verified based on the experimental data from a practical SOFC test bench. The comparative results illustrate that the offline global tuning strategy is effective to calibrate the state-space model and the steady-state model for multiple operation conditions. The online parameter estimation method can capture the slow time-varying behavior of the parameters, while it can be used for single operation condition. Finally, the proposed offline and online parameter estimation methods are efficacy to calibrate the SOFC model.

## Appendix

### A. The model detail of SOFC

The nonlinear functions involved in the voltage balance (1) are expressed as

$$f_1(T_{fc}) = \frac{T_{fc} R}{2F} \ln \left( \frac{P_{H_2} \sqrt{P_{O_2}}}{P_{H_2O}} \right) \quad (42)$$

$$f_2(T_{fc}) = \frac{1}{A_{fc}} e \left[ K_s \left( \frac{1}{T_{fc}} - \frac{1}{T_0} \right) \right] \quad (43)$$

$$f_3(I_{fc}) = \frac{R}{2F} \sinh^{-1} \left( \frac{I_{fc}}{2i_{0,ca} A_{fc}} \right) \quad (44)$$

**Table 5**  
SOFC Model Parameters and coefficients

Symbol	Description	Value
$A_{fc}$	SOFC stack area	38 [cm <sup>2</sup> ]
$E_{act,an}$	anode activation energy	$1 \times 10^4$ [J·mol <sup>-1</sup> ]
$E_{act,ca}$	cathode activation energy	$7 \times 10^4$ [J·mol <sup>-1</sup> ]
$\gamma_{an}$	anode pre-exponential factor	$1.02 \times 10^6$ [A·m <sup>-2</sup> ]
$\gamma_{ca}$	cathode pre-exponential factor	$1.43 \times 10^4$ [A·m <sup>-2</sup> ]
$P_{ref}$	absolute pressure	$1.01325 \times 10^5$ [Pa]
$F$	Faraday's constant	$9.6485 \times 10^4$ [C·mol <sup>-1</sup> ]
$R$	gas constant	$8.3145$ [J·mol <sup>-1</sup> ·K <sup>-1</sup> ]
$T_{an,in}$	anode input gas temperature	623 [K]
$T_{ca,in}$	cathode input gas temperature	623 [K]
$T_{ref}$	reference temperature	25 [°C]
$m_{fc}$	SOFC stack mass	4.3 [kg]
$M_{H_2}$	H <sub>2</sub> molar mass	$2 \times 10^{-3}$ [kg·mol <sup>-1</sup> ]
$M_{H_2O}$	H <sub>2</sub> O molar mass	$18 \times 10^{-3}$ [kg·mol <sup>-1</sup> ]
$M_{O_2}$	O <sub>2</sub> molar mass	$32 \times 10^{-3}$ [kg·mol <sup>-1</sup> ]
$N_{cell}$	number of cells	30
$\Delta H_r^o$	specific heat of reaction	-241.83 [kJ·mol <sup>-1</sup> ]
$T_0$	reference temperature for specific resistance	973 [K]
$I_l$	limiting current	90 [A]
$K_s$	coefficient in the Steinhart-Hart equation	2870

$$f_4(I_{fc}) = \frac{R}{2F} \sinh^{-1} \left( \frac{I_{fc}}{2i_{0,an} A_{fc}} \right) \quad (45)$$

$$f_5(I_{fc}) = \frac{R}{2F} \ln \left( 1 - \frac{I_{fc}}{I_l} \right) \quad (46)$$

where  $P_{H_2}$ ,  $P_{O_2}$  and  $P_{H_2O}$  represents the partial pressure of hydrogen, oxygen and water vapor, respectively.

$$i_{0,ca} = \gamma_{ca} \left( \frac{P_{O_2}}{P_{ref}} \right)^{0.25} e \left( -\frac{E_{act,ca}}{T_{ref} R} \right)$$

$$i_{0,an} = \gamma_{an} \left( \frac{P_{H_2}}{P_{ref}} \right) \left( \frac{P_{H_2O}}{P_{ref}} \right) e \left( -\frac{E_{act,an}}{T_{ref} R} \right)$$

The nonlinear functions for the thermal energy balance (2) are expressed as

$$H^{in} = \sum_{ca} \frac{w_i^{in}}{M_i} \int_{T_{ref}}^{T_{ca,in}} C_{p,i}(T) dT$$

$$+ \sum_{an} \frac{w_i^{in}}{M_i} \int_{T_{ref}}^{T_{an,in}} C_{p,i}(T) dT \quad (47)$$

$$H^r = -\frac{w_{H_2}^r}{M_{H_2}} \Delta H_r^o \quad (48)$$

$$H^{out} = \sum_{an+ca} \frac{w_i^{out}}{M_i} \int_{T_{ref}}^{T_{fc}} C_{p,i}(T) dT \quad (49)$$

## References

- [1] Asghari, S., Mokmeli, A., Samavati, M., 2010. Study of pem fuel cell performance by electrochemical impedance spectroscopy. International Journal of Hydrogen Energy 35, 9283 – 9290.

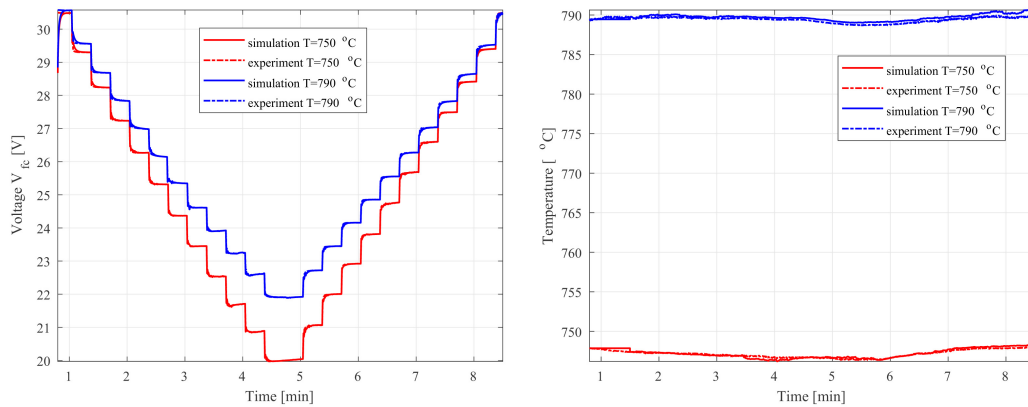


**Figure 9:** The reconstruction results of temperature and voltage by using estimation results of (34).

- [2] Askarzadeh, A., Rezazadeh, A., 2011. Optimization of PEMFC model parameters with a modified particle swarm optimization. *International Journal of Energy Research* 35, 1258–1265. URL: <http://doi.wiley.com/10.1002/er.1787>, doi:10.1002/er.1787.
- [3] Astolfi, A., Ortega, R., 2003. Immersion and invariance: a new tool for stabilization and adaptive control of nonlinear systems. *IEEE Transactions on Automatic control* 48, 590–606.
- [4] Bozorgmehri, S., Hamed, M., 2012. Modeling and Optimization of Anode-Supported Solid Oxide Fuel Cells on Cell Parameters via Artificial Neural Network and Genetic Algorithm. *Fuel Cells* 12, 11–23. URL: <http://doi.wiley.com/10.1002/fuce.201100140>, doi:10.1002/fuce.201100140.
- [5] Chaoui, H., Kandidayeni, M., Boulon, L., Kelouwani, S., Gualous, H., 2021. Real-time parameter estimation of a fuel cell for remaining useful life assessment. *IEEE Transactions on Power Electronics* 36, 7470–7479. doi:10.1109/TPEL.2020.3044216.
- [6] Cheng, J., Zhang, G., 2014. Parameter fitting of PEMFC models based on adaptive differential evolution. *International Journal of Electrical Power and Energy Systems* 62, 189–198. doi:10.1016/j.ijepes.2014.04.043.
- [7] Ettahir, K., Boulon, L., Becherif, M., Agbossou, K., Ramadan, H., 2014. Online identification of semi-empirical model parameters for pemfcs. *International journal of hydrogen energy* 39, 21165–21176.
- [8] Ioannou, P.A., Sun, J., 2012. *Robust adaptive control*. Courier Corporation.
- [9] Jiang, B., Wang, N., Wang, L., 2014. Parameter identification for solid oxide fuel cells using cooperative barebone particle swarm optimization with hybrid learning. *International Journal of Hydrogen Energy* 39, 532–542. doi:10.1016/j.ijhydene.2013.09.072.
- [10] Larminie, J., Dicks, A., McDonald, M.S., 2003. *Fuel cell systems explained*. volume 2. J. Wiley Chichester, UK.
- [11] Li, Q., Chen, W., Wang, Y., Liu, S., Jia, J., 2011. Parameter identification for PEM fuel-cell mechanism model based on effective informed adaptive particle swarm optimization. *IEEE Transactions on Industrial Electronics* 58, 2410–2419. doi:10.1109/TIE.2010.2060456.
- [12] de Mathelin, M., Lozano, R., 1999. Robust adaptive identification of slowly time-varying parameters with bounded disturbances. *Automatica* 35, 1291–1305.
- [13] Murshed, A.M., Huang, B., Nandakumar, K., 2007. Control relevant modeling of planer solid oxide fuel cell system. *Journal of Power Sources* 163, 830–845.
- [14] Na, J., Chen, A.S., Herrmann, G., Burke, R., Brace, C., 2018. Vehicle engine torque estimation via unknown input observer and adaptive parameter estimation. *IEEE Transactions on Vehicular Technology* 67, 409–422. doi:10.1109/TVT.2017.2737440.
- [15] Na, J., Xing, Y., Costa-Castelló, R., 2021. Adaptive estimation of time-varying parameters with application to roto-magnet plant. *IEEE Transactions on Systems, Man, and Cybernetics: Systems* 51, 731–741. doi:10.1109/TSMC.2018.2882844.
- [16] Ohenoja, M., Leiviskä, K., 2010. Validation of genetic algorithm results in a fuel cell model. *International Journal of Hydrogen Energy* 35, 12618–12625. doi:10.1016/j.ijhydene.2010.07.129.
- [17] Outeiro, M.T., Chibante, R., Carvalho, A.S., de Almeida, A.T., 2008. A parameter optimized model of a Proton Exchange Membrane fuel cell including temperature effects. doi:10.1016/j.jpowsour.2008.08.019.
- [18] Peng, J., Huang, J., Wu, X.I., Xu, Y.w., Chen, H., Li, X., 2021. Solid oxide fuel cell (sofc) performance evaluation, fault diagnosis and health control: A review. *Journal of Power Sources* 505, 230058.
- [19] Salim, R., Nabag, M., Noura, H., Fardoun, A., 2015. The parameter identification of the Nexa 1.2kW PEMFC’s model using particle swarm optimization. *Renewable Energy* 82, 26–34. doi:10.1016/j.renene.2014.10.012.
- [20] Schoukens, J., Ljung, L., 2019. Nonlinear system identification: A user-oriented road map. *IEEE Control Systems Magazine* 39, 28–99. doi:10.1109/MCS.2019.2938121.
- [21] Secanell, M., Carnes, B., Suleman, A., Djilali, N., 2007. Numerical optimization of proton exchange membrane fuel cell cathodes. *Electrochimica Acta* 52, 2668–2682. doi:10.1016/j.electacta.2006.09.049.
- [22] Slotine, J.J.E.W.L., 1991. *Applied Nonlinear Control*. Prentice Hall.
- [23] Somaiah, B., Agarwal, V., 2013. Recursive estimation-based maximum power extraction technique for a fuel cell power source used in vehicular applications. *IEEE Transactions on Power Electronics* 28, 4636–4643. doi:10.1109/TPEL.2012.2236688.
- [24] Wu, X., Wang, J., Hao, J., Li, X., 2018. Control of a solid oxide fuel cell stack based on unmodeled dynamic compensations. *International Journal of Hydrogen Energy* 43, 22500–22510.
- [25] Xing, Y., Costa-Castelló, R., Na, J., Renaudineau, H., 2020. Control-oriented modelling and analysis of a solid oxide fuel cell system. *International Journal of Hydrogen Energy* doi:10.1016/j.ijhydene.2020.02.061.
- [26] Yang, J., Li, X., Jiang, J.H., Jian, L., Zhao, L., Jiang, J.G., Wu, X.G., Xu, L.H., 2011. Parameter optimization for tubular solid oxide fuel cell stack based on the dynamic model and an improved genetic algorithm. *International Journal of Hydrogen Energy* 36, 6160–6174. doi:10.1016/j.ijhydene.2011.02.019.
- [27] Ye, M., Wang, X., Xu, Y., 2009. Parameter identification for proton exchange membrane fuel cell model using particle swarm optimization. *International Journal of Hydrogen Energy* 34, 981–989. doi:10.1016/j.ijhydene.2008.11.026.